

Research Article

Effect of Keratin Waste on Poly(ϵ -Caprolactone) Films: Structural Characterization, Thermal Properties, and Keratinocytes Viability and Proliferation Studies

Gianluca Rinaldi , Elena Coccia , Nancy Ferrentino , Chiara Germinario ,
Celestino Grifa , Marina Paolucci , and Daniela Pappalardo 

Department of Science and Technologies, University of Sannio, via de Sanctis snc, Benevento 82100, Italy

Correspondence should be addressed to Marina Paolucci; paolucci@unisannio.it and Daniela Pappalardo; pappalardo@unisannio.it

Received 17 February 2024; Revised 5 April 2024; Accepted 10 April 2024; Published 2 May 2024

Academic Editor: Jun Ling

Copyright © 2024 Gianluca Rinaldi et al. This is an open access article distributed under the Creative Commons Attribution License, which permits unrestricted use, distribution, and reproduction in any medium, provided the original work is properly cited.

Keratin extracted (KE) from chicken feathers was used for the production of composite films comprising poly(ϵ -caprolactone) (PCL) and keratin (PCL/KE films). The process involved the extraction of keratin from chicken feathers using a 0.1 M NaOH solution, followed by characterization via sodium dodecyl sulfate-polyacrylamide gel electrophoresis (SDS-PAGE). The PCL was synthesized through the *ring-opening polymerization* (ROP) of ϵ -caprolactone (ϵ -CL) with Sn(Oct)₂ as a catalyst. Films were prepared via solvent casting, including pure PCL films and those enriched with different weight percentages of KE (10%, 15%, 25%, and 30%). The films were characterized by differential scanning calorimetry (DSC), thermogravimetric analysis (TG), and scanning electron microscopy (SEM). SEM analysis revealed a more uniform incorporation of KE within the PCL matrix in the case of the 15% keratin-enriched film (PCL/KE15) as compared to other keratin percentages. The thermal analysis showed a positive influence of keratin on the thermal stability of the films. Keratinocytes viability and proliferation tests on the PCL/KE15 film demonstrated compatibility with cells. Collectively, these results hold relevance for potential biomedical applications of PCL/KE films.

1. Introduction

Considerable attention has been recently paid to the development of polymeric materials for possible biomedical applications, such as tissue engineering or controlled drug delivery systems [1–4]. In this contest, biodegradable and biocompatible synthetic polymers, such as aliphatic polyesters, emerged in the last decades as predominant in the biomedical field [5]. Among aliphatic polyesters poly(ϵ -caprolactone) (PCL) is extensively used as a polymeric component for tissue regeneration due to its biodegradable and biocompatible nature, excellent mechanical properties, lack of toxicity, and slow degradation rate [6]. PCL is a resorbable polymer; it is degraded *in vivo* by hydrolysis producing hydroxycaproic acid, ultimately removed by urinary excretion and pulmonary elimination as CO₂ [5, 7]. PCL can be industrially prepared by *ring-opening polymerization* (ROP) of ϵ -caprolactone (ϵ -CL), in the presence of stannous (II) 2-ethylhexanoate as a catalyst [8].

Products based on PCL have been in clinical use since early 1990 [5]; however, PCL lacks of functional groups and cell interacting sites, a characteristic that poses a main challenge to researchers aiming for polymeric films or scaffolds capable of recreating the extracellular matrix (ECM) micro-environment to promote tissue repair or regeneration [9, 10].

A possible strategy employed to overcome this limit, and to improve adhesion and cell affinity, consists in blending natural polymers, such as fibrous proteins, into the PCL [11]. Keratin is a fibrous protein found primarily in feathers, hair, wool, animal claws, and fingernails and is among the most abundant proteins in human skin [12]. It is one of the most abundant animal proteins and the main by-product of the wool and poultry industry [13]. The chicken feathers consist of approximately 90% keratin [14]. At a global level, the poultry industry discards every year approximately 7 billion tons of feathers. Such waste is mainly discarded in dumps or transformed into low-quality animal feed, a process that

requires energy-intensive investment [15]. Different methods to valorize the keratin biomass discharge have been reported in the literature [16]; however, new methods of using these wastes are being sought.

Keratin presents advantageous features for biomedical uses. In particular, keratin is rich in some short amino acid sequences, such as arginyl-glycyl-aspartic (RGD), leucine-aspartic acid-valine (LDV), and glutamic acid-aspartic acid-serine (EDS) peptide domains that favor cell adhesion [17]. These peptide domains are well-established cell adhesion sites found in several ECM proteins, including fibronectin [18]. During the healing of cutaneous wounds, keratin, produced by keratinocytes, provides a framework for cell anchoring and regulates keratinocyte proliferation and differentiation [19].

The combination of mammalian keratin with PCL has been already reported in the literature as useful for biomedical applications including tissue engineering [20, 21], vascular engineering [22–24], vascular graft [25], wound healing [26], skin regeneration [27], and bone repair [28]. However, while the use of mammalian keratin with polymers has been largely reported in the literature [29], the combination of chicken keratin with polymeric materials has been studied to a lesser extent. Moreover, when compared with the mammalian keratin, characterized by α -helical secondary structure, the chicken keratin, with its folded-sheet β secondary structure shows superior mechanical properties [30]. Therefore, chicken keratin can be used to fabricate biomaterials that are mechanically more robust than mammalian keratin, while maintaining biocompatibility with mammalian tissues and organs [31]. Chicken feather keratin improved the physical and chemical characteristics of films made with starch [32], chitosan [33], chitosan–starch [34], carrageenan [35], and collagen [36]. On the contrary, the use of chicken feather keratin for the preparation of composite films in combination with synthetic polymers for applications in biomedical field was investigated just in a few cases. In one study, polymeric materials, based on polylactide, were mixed with chicken feather keratin and chitosan, showing promising mechanical behavior and in vitro osteoblast compatibility [37]. In another study, polyurethane and chicken feather keratin were employed to serve as composite scaffolds found to allow fibroblast viability [38]. However, no studies reported the feasibility of blended films with PCL and chicken feather keratin.

Herein, we present the preparation of PCL films enriched with keratin extracted (KE) from chicken feathers. The PCL was synthesized by ROP of ϵ -caprolactone and characterized by NMR and GPC. Films made of pure PCL and keratin-enriched PCL were prepared by solvent casting. The structural and thermal properties of the pure PCL and keratin-enriched PCL films were investigated by DSC, TGA, and SEM. The viability and proliferation of human immortalized keratinocytes (HaCaTs) cultured on PCL/keratin films are reported and discussed.

2. Materials and Methods

2.1. Materials. The polymerization procedure and the manipulation of air-sensitive materials were performed under

nitrogen using Schlenk techniques. The following materials: hexane ($\geq 95\%$), anhydrous toluene (99.8%), stannous octoate $\text{Sn}(\text{Oct})_2$ (92.5%–100.0%), methanol (99.8%), chloroform ($\geq 99.5\%$), Dulbecco's phosphate buffered saline (DPBS), dimethyl sulfoxide (DMSO), and 3-(4,5-dimethylthiazol-2-yl)-2,5-diphenyltetrazolium bromide (MTT) were purchased from Merck (Darmstadt, Germania) and used as received. Sodium hydroxide pellets, sodium dodecyl sulfate (SDS), β -mercaptoethanol, and trichloroacetic acid were purchased from Sigma–Aldrich. The ϵ -caprolactone (ϵ -CL), purchased from Merck, was purified by distillation in vacuo from CaH_2 and stored under nitrogen before use. Precision Plus Protein Dual Color Standards (1610374) and Coomassie Brilliant Blue R-250 were acquired from Bio-Rad (Milan, Italy). The chicken feathers were collected by a local company “Avicola Mauro S.r.l.” (Paolisi, Benevento, Italy). Human immortalized keratinocytes (HaCaTs) were acquired from Cell Lines Service GmbH (Heidelberg, Germany) and cultured in Dulbecco's Modified Eagle Medium (Gibco, Waltham, MA, USA) supplemented with 10% FBS (Merck KGaA, Darmstadt, Germania) and 1% of penicillin/streptomycin solution (10,000 U/mL/10 mg/mL; Gibco, Waltham, MA, USA). The cultures were stored at 37°C, in an atmosphere of 5% CO_2 and 95% humidity.

2.2. Methods

2.2.1. Instruments and Measurements.

(1) Nuclear Magnetic Resonance (NMR). For the NMR spectra, a Bruker AM300 instrument (^1H , 300 MHz; ^{13}C , 75 MHz) was used. Tetramethylsilane (TMS) was used as an internal reference to assign the chemical shifts (^1H and ^{13}C NMR). Chemical shifts were reported as parts per million; coupling constants (J) were reported in Hertz. NMR spectra were indicated also adopting the residual solvent peak at $\delta = 7.27$ (^1H) and at $\delta = 77.16$ (^{13}C) for CDCl_3 . NMR signals were described as follows: chemical shift (δ ppm), relative integral, and multiplicity (s = singlet, d = doublet, t = triplet, q = quartet, m = multiplet, dd = doublet of doublet, and br = broad). The samples were drawn up with a concentration of approximately 10 mg of the compound in 0.5 mL of the deuterated solvent. The software for the recording of the spectra was Bruker TopSpin v3.2. Data processing was obtained by using TopSpin v3.2 or MestReNova v12.0.2 software.

(2) Gel Permeation Chromatography (GPC). The analyses were carried out using the instrument GPC Agilent equipped with a refractive detector and a Plgel 5 μm Mixed-C column. The polymers were dissolved in tetrahydrofuran, filtered through PTFE membranes (0.22 μm), and eluted in tetrahydrofuran. The injection volume was 20.00 μL and the flow rate was 1.00 mL/min. The evaluations were carried out at 35°C according to the temperatures of the columns and detectors. Polystyrene standards with a small molecular weight partitioning were employed as a universal calibration analysis method.

The thermal behavior of samples was investigated by means of simultaneous thermal analyses (thermogravimetry and differential scanning calorimetry, TG/DSC) executed with a NETZSCH STA 449 F3 Jupiter instrument. Thermal

treatment of samples, placed in alumina crucibles, was realized under nitrogen flow (60 mL/min) in the 40–600°C thermal range, with a heating rate of 10°C/min. Data have been processed with NETZSCH Proteus 6.1 software. DSC was used to investigate the melting/recrystallization behavior of samples that underwent two thermal cycles from 40 to 185°C under the same condition of nitrogen flow (60 mL/min) and heating rate (10°C/min). It was possible to determine the melting temperature (T_m), the melting enthalpy (ΔH_m), and the crystallinity degree (X_c). For the PCL, X_c was estimated by the following equation:

$$X_c = \frac{\Delta X_m}{\Delta X_m^0} \times 100, \quad (1)$$

where X_c is the crystallinity degree (%), ΔX_m is the experimental fusion enthalpy (J/g), and ΔX_m^0 is the fusion enthalpy of 100% crystalline PCL (J/g). On the other hand, X_c of the films was estimated by the following equation:

$$X_c = \frac{\Delta X_m}{\Delta X_m^0 (1 - m_f)} \times 100, \quad (2)$$

where X_c is the crystallinity degree (%), ΔX_m is the experimental fusion enthalpy (J/g), ΔX_m^0 is the fusion enthalpy of 100% crystalline PCL (J/g), and m_f is the mass fraction of fiber.

Scanning electron microscopy (SEM) observations were carried out with a Zeiss EVO 15 HD VPSEM operating at 12 and 15 kV accelerating voltage to record images. A double-sided tape was used to fix the samples on aluminum specimen stubs. Samples were then sputtered with a layer of gold with a Q150R ES Sputter Coater (Quorum Technologies, UK).

2.2.2. Keratin Extraction from Chicken Feathers. Chicken waste feathers were cleaned with distilled water and degreased with a solution of SDS at 10%. Feathers were subsequently desiccated in an oven at 60°C for 48 h. Ten grams of feathers were added to 150 mL of 0.1 M NaOH and let soak overnight with stirring. Subsequently, the mixture was filtered with a cotton cloth and the liquid residue was acidified with a 10% trichloroacetic acid solution to adjust the pH at 2.4. The precipitate was gathered and cleaned three times with milli-Q water. The keratin protein sample was stocked at -20°C for 24 hr and then freeze-dried.

The extraction yield of the keratin content from feathers was calculated using Equation (3):

$$Y(\%) = \left[\frac{m_{\text{dry}}}{m_0} \right] \times 100, \quad (3)$$

where m_0 = initial weight of cleaned feathers; m_{dry} = weight of freeze-dried residue.

2.2.3. Sodium Dodecyl Sulfate-PolyAcrylamide Gel Electrophoresis (SDS-PAGE). The molecular weight of the keratin extract (KE) was estimated by SDS-PAGE electrophoresis.

KE was run on 12% polyacrylamide gel under denaturing conditions, as described by Laemmli [39]. Sample preparation was realized based on literature data [13, 40]. Briefly, 35 mg of the KE were dissolved in 1 mL of deionized water and approximately 15 μ L were blended with 5 μ L of loading buffer and boiled for about 10 min. Ten microlitres of protein marker and 20 μ L of denatured KE were loaded into the gel well. The separation was attained at 80 V for 30 min, followed by 120 V for 90 min. Subsequently, the gel was washed twice with distilled water before being stained with Coomassie Brilliant Blue solution. The gel was destained overnight using a solution of 10% glacial acetic acid and 10% methanol. Finally, the gel image was acquired with an imaging instrument (ChemIDoc Imaging System, Bio-Rad, Milan, Italy).

2.3. Polymerization of ϵ -Caprolactone. The synthesis of poly(ϵ -caprolactone) was achieved by ROP of previously distilled ϵ -CL. In a three-neck flask under nitrogen atmosphere, the monomer ϵ -CL (1 mL, 9.0 mmol) and 2.2 mL of a 9 mM solution of Sn(Oct)₂ in toluene were sequentially poured. The obtained solution was thermostated at 130°C with stirring. After 24 h, the polymerization mixture was cooled at room temperature; it was dissolved in the minimum amount of chloroform, and then added to hexane. The precipitated polymer was retrieved by filtration and desiccated in vacuo. Yield = 97%.

¹H NMR (300 MHz, CDCl₃): δ = 4.04 (*t*, 2 H, -(CH₂)₄CH₂O-), 2.29 (*t*, 2 H, -CH₂-C(O)O-), 1.65–1.61 (*m*, 4 H, -CH₂-), 1.39–1.33 (*m*, 2 H, -CH₂-).

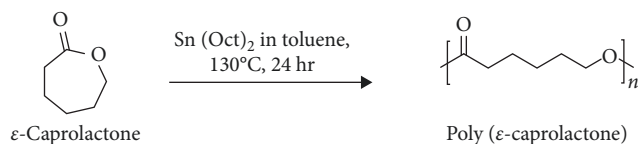
¹³C NMR (75 MHz, CDCl₃): 24.76, 25.72, 28.54, 34.31 (-(COO(CH₂)₄-), 64.33 (-(CH₂)₄CH₂O-), 173.73 (-COO-).

GPC analysis (THF): M_n = 23,200 g/mol; D = 2.0.

2.4. Polymer Film Preparation. Polymer films were prepared by solvent casting technique. Pure poly(ϵ -caprolactone) (PCL) films and PCL films enriched with KE (PCL/KE) were obtained using circular molds with an inner diameter of 1 cm. For the PCL films, the synthesized PCL sample (100 mg) was dissolved in 1.4 mL of chloroform at room temperature with stirring. Thereafter, the solution was poured into the molds with a glass syringe and the solvent was left to evaporate for 24 hr under the fume hood.

PCL/KE were prepared with different keratin concentrations: 10% (PCL/KE10), 15% (PCL/KE15), 25% (PCL/KE25), and 30% (PCL/KE30). The synthesized PCL sample (85 mg) was dissolved in 1.4 mL of chloroform at room temperature with stirring and the keratin powder corresponding to the appropriate percentage was added with magnetic stirring. The mixture was then processed similarly to the pure PCL films. The thicknesses of all the films were measured from images obtained by SEM and are in the range 85–505 μ m (Table S1 and Figure S4).

2.5. In Vitro Cell Culture Study. The viability and proliferation of HaCaTs on PCL and PCL/KE15 films were evaluated by MTT assay [22]. PCL and PCL/KE15 films were placed into a 48-well tissue culture polystyrene plates, sterilized by ultraviolet (UV) irradiation for 30 min, and rinsed rapidly with DPBS containing 1% of penicillin/streptomycin solution [41].



SCHEME 1: Synthesis of poly(ϵ -caprolactone).

Then, HaCaTs were located at a density of 6.0×10^4 cells per well and cultured for time intervals of 1, 3, and 5 days. Forty microlitres of MTT solution (5 mg/mL) were added to each well to evaluate cell viability. After 4 h of incubation in a humidified atmosphere of 5% CO_2 at 37°C for 4 h, the medium was removed and the resulting formazan crystals were dissolved in DMSO by shaking the plates for 15 min in the dark. Finally, absorbance values were calculated at a wavelength of 570 nm with a spectrophotometer (Infinite F200 PRO TECAN, Grödig, Austria). The percentage of cell viability was measured according to Equation (4):

$$\text{Cell viability (\%)} = \frac{100 \times (\text{Abs}_{\text{sample}})}{(\text{Abs}_{\text{control}})}, \quad (4)$$

where $\text{Abs}_{\text{sample}}$ was the absorbance of cells seeded on films and $\text{Abs}_{\text{control}}$ was the absorbance of the HaCat cells incubated in the culture medium [37].

2.6. Statistical Analysis. All experiments were conducted in triplicate. The results were given as mean \pm standard deviation (SD). One-way analysis of variance (ANOVA) was used to evaluate the statistical differences between groups and a Tukey's test was adopted for post hoc analysis. Significant differences were defined as $*p < 0.001$ and $**p < 0.001$. Statistical analysis was achieved using the GraphPad Prism software (version 8.0, San Diego, CA, USA).

3. Results and Discussion

3.1. Synthesis and Characterization of Poly(ϵ -Caprolactone). The synthesis of PCL has been widely reported in the literature [42–46] and was achieved by ROP of ϵ -CL in the presence of Sn(Oct)_2 as a catalyst (Scheme 1). Sn(Oct)_2 has many convenient properties such as high activity, it is easy to handle, inexpensive, and it was approved by the Food and Drug Administration (FDA) as long as used within a limit of 20 ppm of residual tin in medical polymers for commercial purposes [46].

The successful synthesis of the polymer was confirmed by ^1H and ^{13}C NMR. In the ^1H NMR spectrum of the product (solvent CDCl_3 , Figure 1), the characteristic chemical shifts at 1.36, 1.65–1.61, 2.29, and 4.04 ppm of the PCL were observed. The ^{13}C NMR spectrum in CDCl_3 (Figure S1, see Supporting Information) showed characteristic signals at 24.76, 25.72, 28.54, 34.31, 64.33, 173.73 ppm. Macromolecular weight and macromolecular weight distribution of the polymer were determined by GPC in THF and resulted respectively $M_n = 23,200$ g/mol and $\bar{D} = 2.0$ (Figure S2, see Supplementary Materials). The origin of the observed dispersity value can be related to

the used catalyst, Sn(Oct)_2 , which could promote transesterification reactions [47].

DSC analyses were carried out to assess the melting and crystallization behavior of the polymer. The resulting enthalpic curve shows a distinct melting peak at 60.7°C , during the second heating scan (see Table S2 in the Supplementary Materials).

To evaluate the thermal stability of the polymer, thermogravimetric analysis (TG) was performed, and the resultant thermal data were summarized in Table 1. The weight loss of the synthesized PCL, under a controlled nitrogen-flow environment, was plotted as a function of temperature in Figure S3 (Supplementary Materials). The onset of degradation was identified at approximately 300°C . It is noteworthy that a singular degradation step, characterized by an inflection point at 338.3°C , was observed in the degradation process. This observation aligns with existing literature on PCL samples, despite the slightly lower initiation temperature in our case [48]. The observed variation in degradation temperature can be attributed to differences in the molecular weights of the compared samples. It is well-known that the molecular weight of PCL exerts a significant influence on its degradation behavior [49].

3.2. Keratin Extract from Chicken Feathers. Several methods for keratin extraction are described in the literature, ranging from acidic and alkaline hydrolysis to *inter*- and *intra*-molecular disulfide bond breaking [50], as well as reduction and oxidation methods or enzymatic hydrolysis [51]. Most of these methods are based on the use of organic solvents, and/or other chemicals such as sodium sulfide, metabisulphite, and 2-mercaptoethanol [52]. However, the involvement of chemicals and organic solvents for the keratin extraction is not only associated with high costs but has a significant environmental impact [52, 53]. With the aim of reducing the environmental impact of the extraction method, in this study the extraction was performed by alkaline hydrolysis [54]. Although the extraction yield is quite low, this method avoids organic solvents and harmful chemicals and ensures less damage to keratin amino acids than acidic hydrolysis [52]. The extraction was carried out using a basic aqueous solution of 0.1 M NaOH. The yield was 16%, which was satisfactory considering that the yield is dependent on the processing conditions, and the feathers were used as they were, without a pretreatment [53, 55–57]. The results of the SDS-PAGE analysis on a 12% polyacrylamide gel, for the determination of the molecular weight of the KE, are reported in Figure 2. Two bands corresponding to about 10 and 20 kDa are visible. This outcome is in agreement with the literature, reporting one band of about 10 kDa, representing the not-dimerized form, and a band of about 20 kDa, representing the dimerized form, confirming the ability of this protein to self-assemble into a dimer [29].

The results of the thermogravimetric analysis shown in Figure 3 indicate a gradual degradation of KE, resulting in a total weight loss of 69.9% (Table 1). The first peak at 73.8°C on the DTG curve can be attributed to the evaporation of water bound to keratin through physical interactions and hydrogen bonds [50], whereas the thermal degradation of

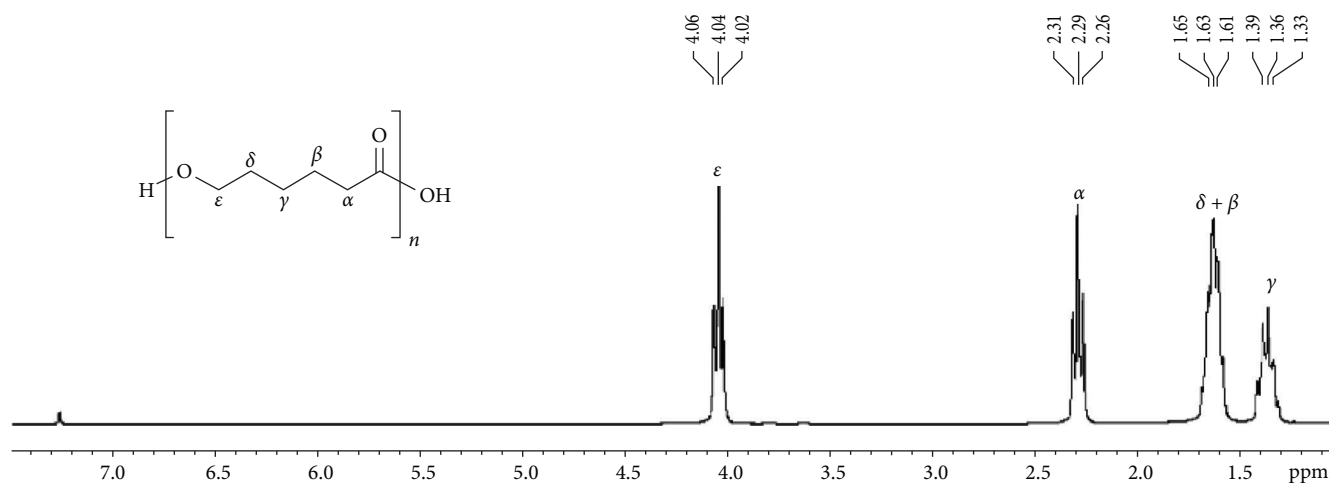


FIGURE 1: ^1H NMR spectrum (300 MHz, CDCl_3 , 298 K) of poly(ϵ -caprolactone).

TABLE 1: Thermal behavior of PCL, KE, PCL/KE10, PCL/KE15, PCL/KE25, and PCL/KE30 films analyzed by TG-DSC analyses.

Sample	<200°C			200–450°C			450–600°C			TWL	RM
	ΔW (%)	DTG (°C)	DSC (°C)	ΔW (%)	DTG (°C)	DSC (°C)	ΔW (%)	DTG (°C)	DSC (°C)		
PCL	0.2	—	63.8 ^a	98.4	338.3	343.4 ^a	0.3	—	—	98.9	1.1
KE	4.2	68.5–145.5	65.3 ^a	58.9	281.5–330.5	223.9 ^b –339.6 ^a	6.8	517.0	519.4 ^a	69.9	30.1
PCL/KE10	1.1	—	59.1 ^a	96.7	340.6–378.9	342.6 ^a –352.1 ^a –378.9 ^a	1.7	—	492.1 ^a	99.4	0.6
PCL/KE15	0.8	—	63.3 ^a	90.1	350.3–391.8	354.7 ^a –394.3 ^a	1.8	—	520.2 ^a	92.7	7.3
PCL/KE25	1.4	—	59.3 ^a	93.7	345.5–386.2	345.0 ^a –362.0 ^a –387.5 ^a	2.6	—	498.6 ^a	97.7	2.4
PCL/KE30	1.1	—	59.1 ^a	91.0	346.2–388.4	355.2 ^a –391.7 ^a	2.1	—	491.3 ^a	94.1	5.9

ΔW = weight loss (by TG); TWL = total weight loss; RM = residual mass. ^aEndothermic reaction; ^bexothermic reaction.

keratin fiber was observed in the range between 200 and 450°C, with a peak on a DTG curve at 330.5°C (Figure 3). This behavior is in agreement with the literature data [50]. Above 450°C the weight loss (6.8 wt.%) is due to the advanced degradation of keratin structure at high temperature [58].

3.3. Films Characterization. Pure PCL films and PCL films enriched with KE (PCL/KE) were prepared by solvent casting. For the PCL/KE films, different keratin concentrations were selected: 10% (PCL/KE10), 15% (PCL/KE15), 25% (PCL/KE25), and 30% (PCL/KE30).

The characterization of pure PCL and PCL/KE films was achieved by means of simultaneous thermal analyses (TA) and SEM. Thermogravimetric analysis of the samples was performed in a nitrogen atmosphere by heating the samples from 40 to 600°C. The TG and DTG curves of PCL/KE, pure PCL, and KE films are shown in Figure 4. For all samples, the data of thermal behavior and temperature degradation range are summarized in Table 1.

It is worth noting that all PCL/KE films exhibited superior thermal stability compared to both PCL and KE films.

The incorporation of keratin into the PCL matrix resulted in an enhancement of the thermal stability of the PCL/KE films. Among these films, the PCL/KE15 variant displayed a slightly higher level of thermal stability when compared to the other PCL/KE films (see Table 1 and Figure 4). The thermal degradation of the films can be broadly categorized into three stages: the initial stage ($T < 200^\circ\text{C}$) primarily involved the evaporation of water molecules. In this phase, all PCL/KE films exhibited approximately 1% weight loss, whereas the pure PCL film exhibited notably lower weight loss. This variation in weight loss is attributed to the presence of water in the PCL/KE films, stemming from the inherent hydrophilic nature of KE. The subsequent stage involved the thermal degradation of the films. Both pure PCL and PCL/KE films demonstrated similar final thermal degradation temperatures, with nearly complete degradation occurring at approximately 450°C. The final stage, characterized by a weight loss of less than 3% in the PCL/KE films, was attributed to the advanced degradation of the keratin component. Regarding the melting behavior, DSC measurements revealed that the melting temperature, recorded during the second heating scan, was higher for the pure PCL film

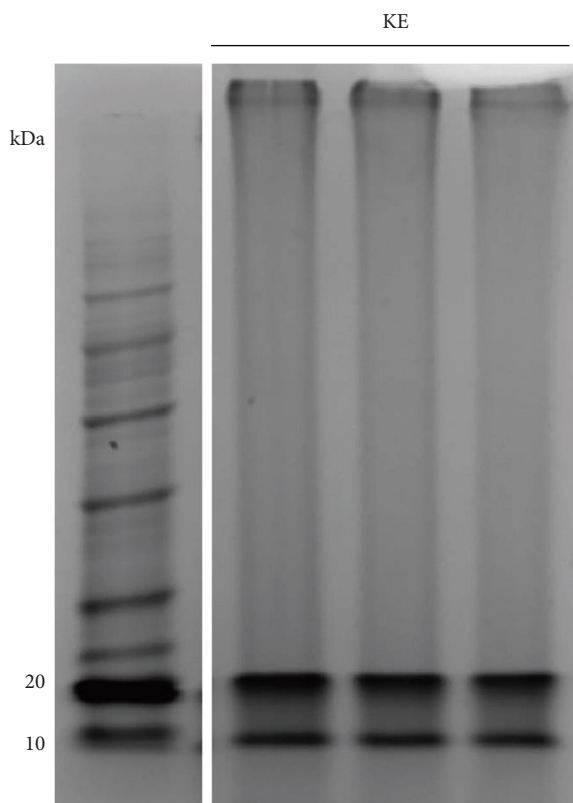


FIGURE 2: SDS-PAGE of keratin extract (KE). The left line is the molecular marker. kDa, kilodalton; KE, keratin extract.

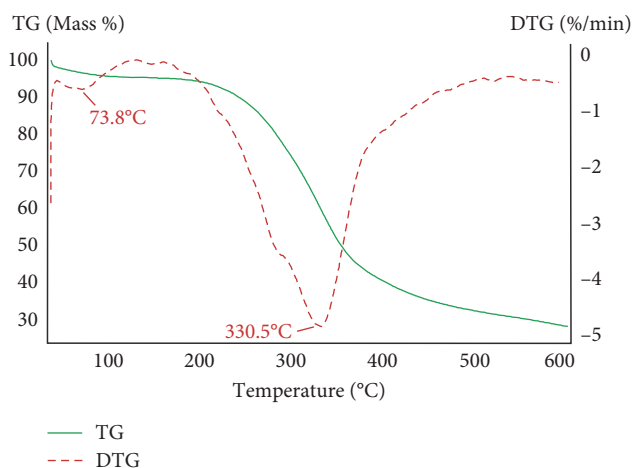


FIGURE 3: Thermogravimetric curve (TG) and first derivative of TG curve (DTG) of keratin extract (KE) sample.

(60.7°C) compared to the temperatures observed for the PCL/KE films (ranging from 54.8 to 57.8°C) (Figure 5; Table S2). Additionally, the melting enthalpy (ΔH_m) value for the second heating scan of the PCL/KE films was lower than that of the pure PCL film. The same trend was observed for the crystallinity degree [59] (Table S2, Supplementary Materials). Notably, the ΔH_m value observed for the PCL/KE15 sample appeared to be higher than that of the other films, warranting closer examination.

PCL/KE films were also characterized by SEM, along with KE and pure PCL film (Figure 6). The keratin powder was composed of fibers of different sizes (Figure 6(a)). The pure PCL film, obtained by solvent casting, showed a smooth and microcracked surface, likely due to the evaporation of the solvent during the preparation process (Figure 6(b)).

SEM images revealed a partial arrangement of KE unevenly distributed on the surface of the PCL/KE10 film (Figure 6(c)), whereas on the PCL/KE15 sample, a more homogeneous incorporation of KE with a uniform distribution was observed (Figure 6(d)). By contrast, the distribution of KE appeared not uniform in both PCL/KE25 (Figure 6(e)) and PCL/KE30 (Figure 6(f)), which released unincorporated keratin, overlaid on the polymeric film.

SEM observations of the cut surfaces revealed interesting information (Figure 7). While the pure PCL appeared smooth and compact (Figure 7(a)), the cut surface of PCL/KE15 was rough and jagged (Figure 7(b)). This aspect might have a positive effect in biomedical application of the films, e.g., as medical patch on the wound healing process. The microarchitecture of the films, in fact, is of fundamental importance in the interactions between the cells and the polymeric materials, as the cells perceive the characteristics of the local geometry [60]. Based on these advantageous features, PCL/KE15 was therefore selected for cell viability and proliferation tests.

3.4. HaCaTs Viability and Proliferation Study. In vitro cell viability and proliferation tests were conducted on the human epidermal keratinocyte line (HaCaTs). HaCaTs viability and proliferation were detected by MTT assay. The MTT method is a colorimetric test that measures the cellular metabolic activity, as an indirect measure of cytotoxicity. Indeed, MTT (3-(4,5-dimethylthiazol-2-yl)-2,5-diphenyltetrazolium bromide) enters live cells through endocytosis and it is reduced to blue formazan by mitochondrial enzymes [51], a process only possible in viable cells [61].

As reported in Figure 8, HaCaTs cultured on both PCL films and those enriched with different weight percentages of KE (10%, 15%, 25%, and 30%) were viable during the culture period (5 days). In particular, HaCaTs cultured on pure PCL films did not show any significant differences with regard to the control, without film, on day 1, while significant differences were observed in cell proliferation rates on days 3 and 5 [28]. The HaCaTs cultured on PCL films enriched with different weight percentages of KE showed significant differences with regard to the control, without film, on days 1, 3, and 5. The highest proliferation rate was recorded in HaCaTs grown on PCL/KE15 films since day 1. However, the cell growth rate from days 3 to 5 was slower than that from days 1 to 3, likely due to insufficient space and nutrients, which limited the cell proliferation [28].

Our results are in consonance with the current literature reporting the nontoxicity of PCL and PCL/KE films and scaffolds as well as a certain growth and proliferation-promoting effect [11, 28, 37]. Interestingly, in this study, PCL/KE films showed a positive effect on cell growth and proliferation starting from day 1 of incubation, while studies in the literature report cell viability and an increase in

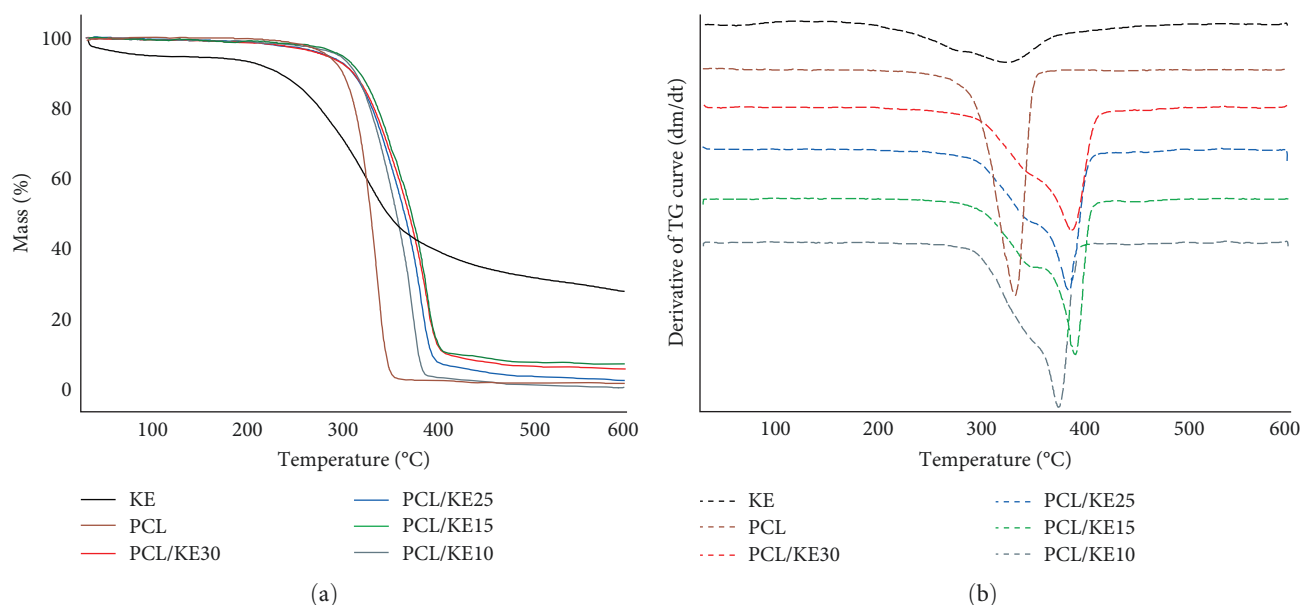


FIGURE 4: Thermogravimetric curve (TG) (a) and first derivative of TG curve (DTG) curves (b) of pure polycaprolactone (PCL), keratin extract (KE), and PCL/KE films.

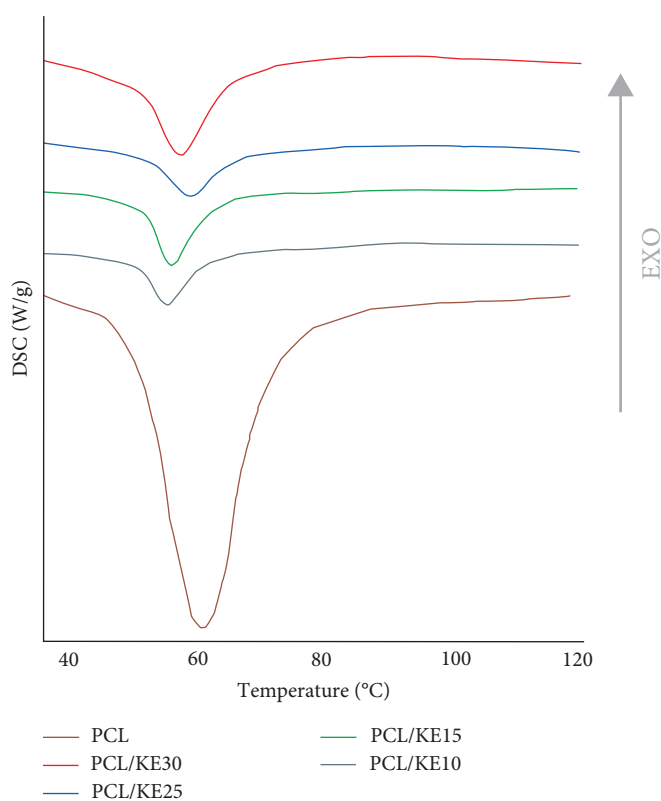


FIGURE 5: Differential scanning calorimetry (DSC) curves of PCL and PCL/KE films.

proliferation in PCL/keratin scaffolds only from day 3. Moreover, in previous literature reports both polyester film alone and enriched with keratin gave the same results, indicating that the addition of keratin had only a limited effect on cell growth and proliferation [11, 28, 37]. The higher positive effect due to the keratin addition may be due to the kind of

keratin used. Indeed, our films were manufactured with keratin from chicken feathers, while in previous reported studies keratin derived from wool or human hair was used [11, 28]. Keratins can be distinguished in α and β types [13], exhibiting also different filament-matrix structures at nanoscale size; while β -keratin filaments have a diameter of 3–4 nm [62], α -keratin filaments have a diameter of 7 nm [13]. Interestingly, human hair and wool contain α -keratin, while feathers contain β -keratin [63]. Therefore, we may hypothesize that the different structures of the β -keratins promoted cell adhesion and proliferation, explaining why HaCaTs proliferation on PCL/KE films started as early as day 1. In fact, the β -sheet structure of keratin provides a more favorable substrate and more stable scaffold for cells adhesion than the alpha conformation [63]. The 3D structure of β -keratin facilitates the migration of cells within the matrix, allowing them to effectively colonize the scaffold and contribute to the formation of new tissue [29]. This is essential for tissue regeneration where cells must move and interact with each other to restore the functionality of damage tissue. The highest cell growth rates observed for PCL/KE15 films are most likely due to the higher homogeneously incorporated concentration of keratin in the films. Although PCL/KE25 and PCL/KE30 contain the highest weight percentages of keratin, it is not all incorporated homogeneously into the films, as demonstrated by SEM analyses, and, therefore, is not able to provide the necessary support to promote growth of cells.

4. Conclusions

The use of PCL in several biomedical applications, such as tissue engineering, is strongly hampered by the lack of cell recognition sites, which could mimic the ECM microenvironment to promote tissue repair or regeneration. In this study, we have used keratin, a fibrous protein, which is

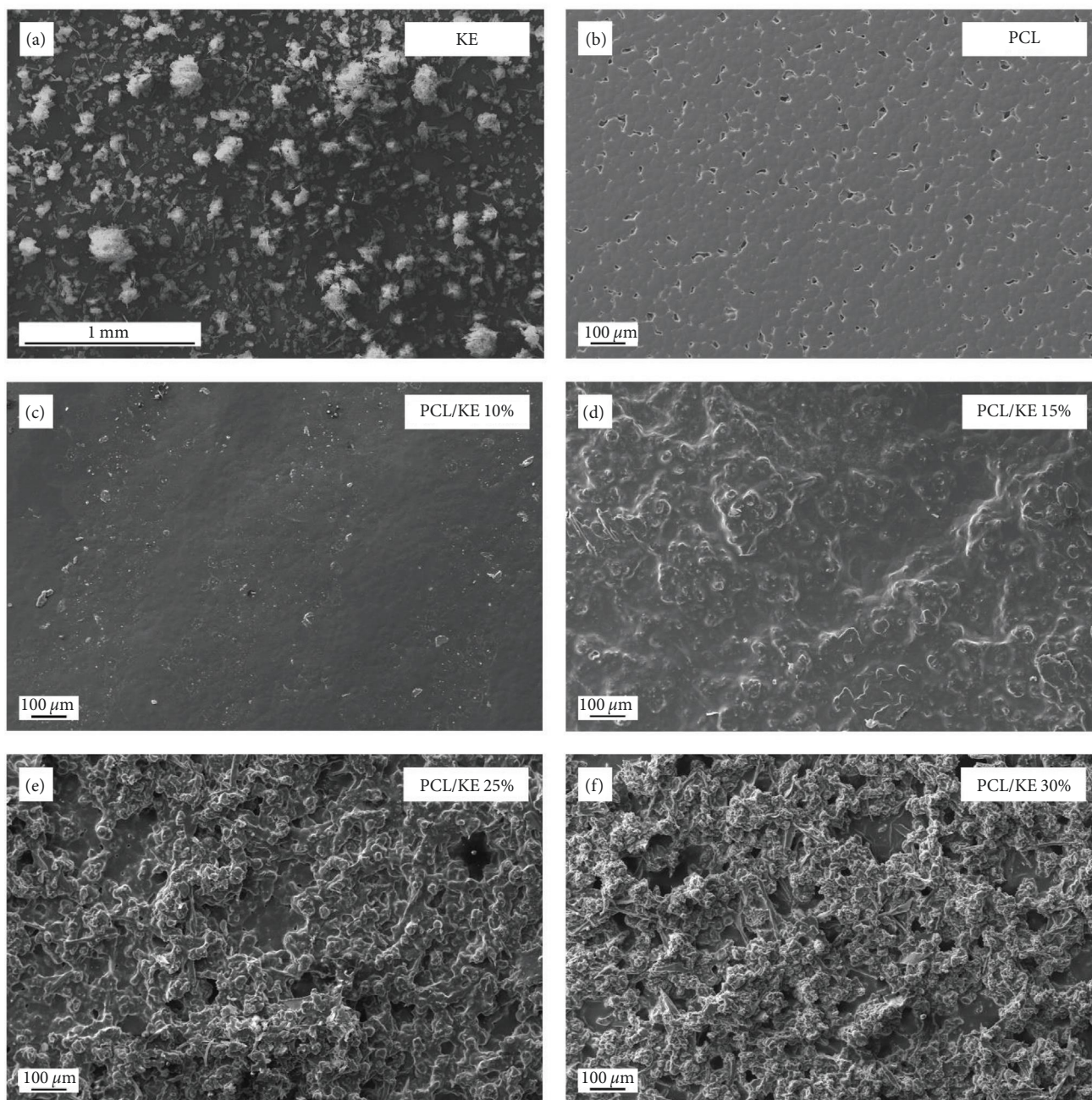


FIGURE 6: Scanning electron microscopy images of (a) KE, (b) PCL, (c) PCL/KE10, (d) PCL/KE15, (e) PCL/KE25, and (f) PCL/KE30.

rich in cell adhesion sequences, to produce KE-enriched polymeric films (PCL/KE) with various percentages.

Keratin biomaterials, both of bird and mammalian origin, have been largely studied in the context of tissue regeneration biomaterials for wound healing [64]. A survey of the literature showed several studies on PCL or KE, but, to the best of our knowledge, this specific combination, i.e., KE from chicken feathers and PCL, was not used before. Previous studies used chicken feathers keratin in combination with carrageenan materials [35] or polyurethanes [38] to

obtain films. In our approach, the films are obtained by using a biodegradable and biocompatible aliphatic polyester, such as PCL, to increase the performance of films which therefore have, as an added value, the biodegradability and resorbability of the polymer. Other authors, instead, used films made of PCL and keratin, by using mammalian KE from wool [65]. Again, the combination of PCL and mammalian keratin has been used for the formation of hydrogels [66]. Polymeric films made of aliphatic polyesters other than PCL have also been prepared and fibroblasts adhesion studies were carried

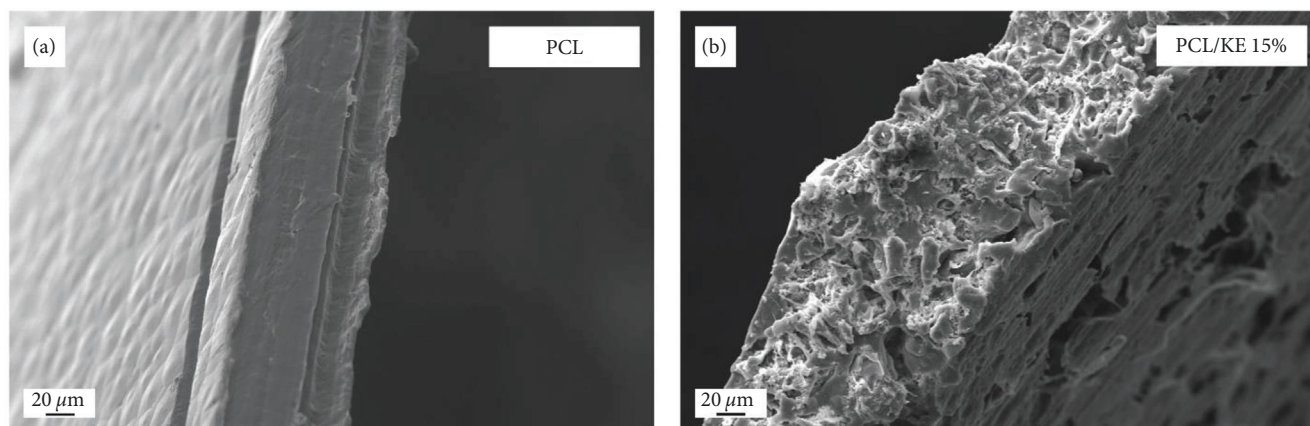


FIGURE 7: Scanning electron microscopy images of (a) cross-section of pure PCL film; (b) cross-section of PCL/KE15 film.

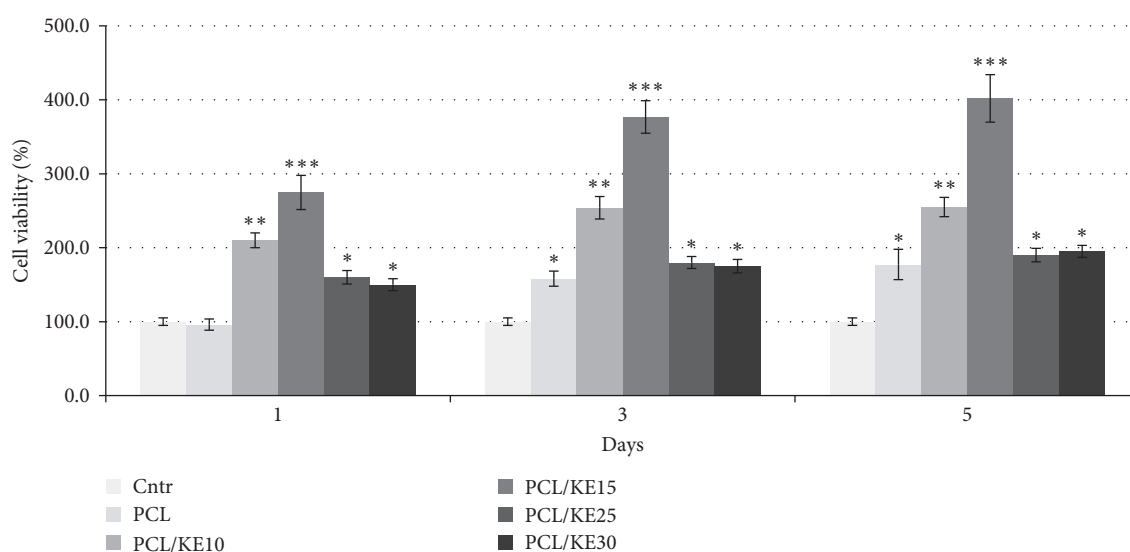


FIGURE 8: Viability and proliferation of HaCaTs grown on PCL films and PCL/KE films (10%, 15%, 25%, and 30%) measured by MTT assay after 1, 3, and 5 days. Data represent means \pm SD. Significant differences from control were defined as * $p < 0.01$, ** $p < 0.001$, and *** $p < 0.0001$.

out [41]. Our study represents an advance in biodegradable materials research thanks to the innovative combination of PCL and keratin (KE) derived from chicken feathers.

The addition of KE from chicken feathers to PCL films affected the thermal properties. In particular, the KE-enriched films had a higher thermal stability when compared to their pure PCL counterparts. The results of the HaCaTs viability on the PCL/KE15 films were also very promising. Indeed, cell viability evaluated over a period of 5 days was higher than reported in previous studies where mammalian keratin derived from wool or human hair was used. This encouraging result could be explained by the kind of keratin used here. In particular, in our film, the β keratin derived from chicken feathers was used, the previously used keratin was the mammalian one, which is mainly constituted by α keratin filaments. Further studies will be needed to support this hypothesis and to compare the effect of the β keratin derived from chicken feathers with respect to the mammalian α keratin in analogous conditions, i.e., by using the

identical extraction method and identical polymeric PCL matrix. The results are promising and encourage the search in this field.

The PCL/KE enriched materials may have promising application in the biomedical fields, i.e., in tissue engineering application, where PCL has been already largely applied as wound healing material. The presence of KE may increase the cell-materials interactions respect to the pure PCL and may favor the proliferation of cells. As a result, the PCL/KE films could have potential applications in the biomedical field, e.g., as patch for the wound healing process.

Data Availability

The data used to support the findings of this study are available from the corresponding authors upon request.

Conflicts of Interest

The authors declare that they have no conflicts of interest.

Acknowledgments

The authors gratefully acknowledge Dr. Graziella Orso for SDS-PAGE analysis technical support. This work was supported by University of Sannio funding (FAR 2021) and PRIN PNNR “New recyclable thermosetting and elastomeric polymeric materials based on bio-renewable feedstocks” (CUP F53D23009010001).

Supplementary Materials

The following data and figures are included as supplementary materials: ^{13}C NMR spectrum of the PCL sample; GPC curve and TGA analysis of the PCL sample (Figures S1–S3); Table S1 summarizing thickness of PCL, PCL/KE10, PCL/KE15, PCL/KE25, and PCL/KE30 films; Table S2 summarizing the thermal behavior data by DSC analyses of all the films; images of all the films obtained by SEM (Figure S4). (*Supplementary Materials*)

References

- [1] R. Ravichandran, S. Sundarajan, J. R. Venugopal, S. Mukherjee, and S. Ramakrishna, “Advances in polymeric systems for tissue engineering and biomedical applications,” *Macromolecular Bioscience*, vol. 12, no. 3, pp. 286–311, 2012.
- [2] R. Song, M. Murphy, C. Li, K. Ting, C. Soo, and Z. Zheng, “Current development of biodegradable polymeric materials for biomedical applications,” *Drug Design, Development and Therapy*, vol. 12, 2018.
- [3] P. K. Deb, S. F. Kokaz, S. N. Abed, A. Paradkar, and R. K. Tekade, “Chapter 6—pharmaceutical and biomedical applications of polymers,” *Basic Fundamentals of Drug Delivery*, pp. 203–267, 2019.
- [4] S. Jadoun, U. Riaz, and V. Budhiraja, “Biodegradable conducting polymeric materials for biomedical applications: a review,” *Medical Devices & Sensors*, vol. 4, no. 1, 2021.
- [5] D. Pappalardo, T. Mathisen, and A. Finne-Wistrand, “Biocompatibility of resorbable polymers: a historical perspective and framework for the future,” *Biomacromolecules*, vol. 20, no. 4, pp. 1465–1477, 2019.
- [6] S. A. Sell, P. S. Wolfe, K. Garg, J. M. McCool, I. A. Rodriguez, and G. L. Bowlin, “The use of natural polymers in tissue engineering: a focus on electrospun extracellular matrix analogues,” *Polymers*, vol. 2, no. 4, pp. 522–553, 2010.
- [7] C. G. Pitt, F. I. Chasalow, Y. M. Hibionada, D. M. Klimas, and A. Schindler, “Aliphatic polyesters. I. The degradation of poly (ϵ -caprolactone) in vivo,” *Journal of Applied Polymer Science*, vol. 26, 1981.
- [8] A.-C. Albertsson and I. K. Varma, “Recent developments in ring opening polymerization of lactones for biomedical applications,” *Biomacromolecules*, vol. 4, no. 6, pp. 1466–1486, 2003.
- [9] M. Heidari, S. H. Bahrami, M. Ranjbar-Mohammadi, and P. B. Milan, “Smart electrospun nano fibers containing PCL/gelatin/graphene oxide for application in nerve tissue engineering,” *Materials Science & Engineering C*, vol. 103, 2019.
- [10] K. L. Christman, “Regenerative medicine: biomaterials for tissue repair,” *Science*, vol. 363, 2019.
- [11] W. S. Choi, J. H. Kim, C. B. Ahn et al., “Development of a multi-layer skin substitute using human hair keratinic extract-based hybrid 3d printing,” *Polymers*, vol. 13, no. 16, Article ID 2584, 2021.
- [12] R. Moll, M. Divo, and L. Langbein, “The human keratins: biology and pathology,” *Histochemistry and Cell Biology*, vol. 129, pp. 705–733, 2008.
- [13] J. Wang, S. Hao, T. Luo, Q. Yang, and B. Wang, “Development of feather keratin nanoparticles and investigation of their hemostatic efficacy,” *Materials Science and Engineering: C*, vol. 68, pp. 768–773, 2016.
- [14] A. Grazziotin, F. A. Pimentel, E. V. de Jong, and A. Brandelli, “Nutritional improvement of feather protein by treatment with microbial keratinase,” *Animal Feed Science and Technology*, vol. 126, no. 1-2, pp. 135–144, 2006.
- [15] T. K. Kumawat, A. Sharma, A. Sharma, and S. Chandra, “Keratin waste: the biodegradable polymers,” *Polymers*, 2018.
- [16] C. C. Reddy, I. A. Khilji, A. Gupta et al., “Valorization of keratin waste biomass and its potential applications,” *Journal of Water Process Engineering*, vol. 40, Article ID 101707, 2021.
- [17] Y. Wang, W. Zhang, J. Yuan, and J. Shen, “Differences in cytocompatibility between collagen, gelatin and keratin,” *Materials Science & Engineering C*, vol. 59, pp. 30–34, 2016.
- [18] V. Singh, S. Wang, and K. W. Ng, “2.25 keratin as a biomaterial,” *Comprehensive Biomaterials II*, vol. 2, 2017.
- [19] J. Frank, F. K. Jugert, H. F. Merk et al., “A spectrum of novel mutations in the protoporphyrinogen oxidase gene in 13 families with variegate porphyria,” *Journal of Investigative Dermatology*, vol. 116, no. 5, pp. 821–823, 2001.
- [20] A. Edwards, D. Jarvis, T. Hopkins, S. Pixley, and N. Bhattarai, “Poly (ϵ -caprolactone)/keratin-based composite nanofibers for biomedical applications,” *Journal of Biomedical Materials Research—Part B Applied Biomaterials*, vol. 103, no. 1, pp. 21–30, 2015.
- [21] P. Wu, X. Dai, K. Chen, R. Li, and Y. Xing, “Fabrication of regenerated wool keratin/polycaprolactone nanofiber membranes for cell culture Panpan,” *Biological Macromolecules*, 2018.
- [22] Y. Li, Y. Wang, J. Ye, J. Yuan, and Y. Xiao, “Fabrication of poly (ϵ -caprolactone)/keratin nanofibrous mats as a potential scaffold for vascular tissue engineering,” *Materials Science and Engineering: C*, vol. 68, pp. 177–183, 2016.
- [23] W. Xiuzhen, W. Yanfang, J. Xingxing, L. Pengfei, Y. Jiang, and S. Jian, “Heparinized PCL/keratin mats for vascular tissue engineering scaffold with potential of catalytic nitric oxide generation,” *Journal of Biomaterials Science Polymer Edition*, vol. 29, no. 14, 2018.
- [24] J. Dou, Y. Wang, X. Jin et al., “PCL/sulfonated keratin mats for vascular tissue engineering scaffold with potential of catalytic nitric oxide generation,” *Materials Science & Engineering C*, vol. 107, 2020.
- [25] X. Li, Y. Wei, S. Jiang et al., “Full bio-based soy protein isolate film enhanced by chicken feather keratin,” *Macromolecular Materials and Engineering*, vol. 306, no. 5, 2021.
- [26] X. Deng, M. Gould, and M. A. Ali, “Fabrication and characterisation of melt-extruded chitosan/keratin/PCL/PEG drug-eluting sutures designed for wound healing,” *Materials Science & Engineering C*, vol. 120, Article ID 111696, 2021.
- [27] M. Ranjbar-mohammadi, “Designing hybrid nanofibers based on keratin-poly (vinyl alcohol) and poly for application as wound dressing,” *Journal of Industrial Textiles*, vol. 51, pp. 1–21, 2021.
- [28] L. Sun, S. Li, K. Yang, J. Wang, Z. Li, and N. Dan, “Polycaprolactone strengthening keratin/bioactive glass composite scaffolds with double cross-linking networks for potential application in bone repair,” *Journal of Leather Science and Engineering*, vol. 4, no. 1, 2022.

- [29] B. S. Lazarus, C. Chadha, A. Velasco-Hogan, J. D. V. Barbosa, I. Jasiuk, and M. A. Meyers, "Engineering with keratin: a functional material and a source of bioinspiration," *iScience*, vol. 24, no. 8, Article ID 102798, 2021.
- [30] Y. Esparza, N. Bandara, A. Ullah, and J. Wu, "Hydrogels from feather keratin show higher viscoelastic properties and cell proliferation than those from hair and wool keratins," *Materials Science and Engineering: C*, vol. 90, pp. 446–453, 2018.
- [31] S. Feroz, N. Muhammad, J. Ratnayake, and G. Dias, "Based materials for biomedical applications," *Bioactive Materials*, vol. 5, no. 3, pp. 496–509, 2020.
- [32] O. M. Oluba, C. F. Obi, O. B. Akpor et al., "Fabrication and characterization of keratin starch biocomposite film from chicken feather waste and ginger starch," *Scientific Reports*, vol. 11, no. 1, 2021.
- [33] B. Khanzada, B. Mirza, and A. Ullah, "Chitosan based biocomposites packaging films with unique mechanical and barrier properties," *Food Packaging and Shelf Life*, vol. 35, Article ID 101016, 2023.
- [34] C. G. Flores-Hernández, A. Colin-Cruz, C. Velasco-Santos et al., "Chitosan–starch–keratin composites: improving thermo-mechanical and degradation properties through chemical modification," *Journal of Polymers and the Environment*, vol. 26, no. 5, pp. 2182–2191, 2018.
- [35] A. You, M. Be, and I. In, "Synthesis and characterization of keratin hydrolisate–carrageenan biofilm," *AIP Conference Proceedings*, vol. 2296, no. 1, 2023.
- [36] S. Balaji, R. Kumar, R. Sriprya et al., "Characterization of keratin–collagen 3D scaffold for biomedical applications," *Polymers for Advanced Technologies*, vol. 23, no. 3, pp. 500–507, 2012.
- [37] C. E. Tanase and I. Spiridon, "PLA/chitosan/keratin composites for biomedical applications," *Materials Science and Engineering: C*, vol. 40, pp. 242–247, 2014.
- [38] O. Gokce, M. Kasap, G. Akpinar, and G. Ozkoc, "Preparation, characterization, and *in vitro* evaluation of chicken feather fiber–thermoplastic polyurethane composites," *Journal of Applied Polymer Science*, vol. 134, no. 45, 2017.
- [39] U. Laemmli, "Cleavage of structural proteins during the assembly of the head of bacteriophage T4," *Nature*, vol. 227, pp. 680–685, 1970.
- [40] O. D. Fagbemi, B. Sithole, and T. Tesfaye, "Optimization of keratin protein extraction from waste chicken feathers using hybrid pre-treatment techniques," *Sustainable Chemistry and Pharmacy*, vol. 17, Article ID 100267, 2020.
- [41] S. Braccini, G. Pecorini, F. Chiellini, D. Bakos, S. Miertus, and V. Frecer, "Adhesion of fibroblast cells on thin films representing surfaces of polymeric scaffolds of human urethra rationalized by molecular models of integrin binding: cell adhesion on polymeric scaffolds for regenerative medicine," *Journal of Biotechnology*, vol. 324, pp. 233–238, 2020.
- [42] S. I. Erdagi, E. Doganci, C. Uyanik, and F. Yilmaz, "Heterobifunctional poly(ϵ -caprolactone): Synthesis of α -cholesterol- ω -pyrene PCL via combination of ring-opening polymerization and "click" chemistry," *Reactive and Functional Polymers*, vol. 99, pp. 49–58, 2016.
- [43] Z. M. Ahin, E. Doanci, S. Z. Yildiz et al., "Synthesis and characterization of two-armed poly(ϵ -caprolactone) polymers initiated by the Schiff's base complexes of copper(II) and nickel(II)," *Synthetic Metals*, vol. 160, no. 17–18, pp. 1973–1980, 2010.
- [44] E. Doganci, M. A. Tasdelen, and F. Yilmaz, "Synthesis of miktoarm star-shaped polymers with POSS core via a combination of CuAAC click chemistry, ATRP, and ROP techniques," *Macromolecular Chemistry and Physics*, vol. 216, no. 17, pp. 1823–1830, 2015.
- [45] A. Uner, E. Doganci, and M. A. Tasdelen, "Non-covalent interactions of pyrene end-labeled star poly(ϵ -caprolactone)s with fullerene," *Journal of Applied Polymer Science*, vol. 135, no. 29, pp. 1–8, 2018.
- [46] G. Gorrasi, L. Vertuccio, L. Annunziata, C. Pellicchia, and D. Pappalardo, "Correlations between microstructural characterization and thermal properties of well defined poly(ϵ -caprolactone) samples by ring opening polymerization with neutral and cationic bis(2,4,6-triisopropylphenyl)tin(IV) compounds," *Reactive and Functional Polymers*, vol. 70, no. 3, pp. 151–158, 2010.
- [47] H. R. Kricheldorf, J. M. Jonté, and M. Berl, "Polylactones 3. Copolymerization of glycolide with L, L-lactide and other lactones," *Die Makromolekulare Chemie*, vol. 12, no. S19851, pp. 25–38, 1985.
- [48] M. Unger, C. Vogel, and H. W. Siesler, "Molecular weight dependence of the thermal degradation of poly(ϵ -caprolactone): a thermogravimetric differential thermal fourier transform infrared spectroscopy study," *Applied Spectroscopy*, vol. 64, no. 7, pp. 805–809, 2010.
- [49] A. Sorrentino, G. Gorrasi, V. Bugatti, T. Fuoco, and D. Pappalardo, "Polyethylene-like macrolactone-based polyesters: rheological, thermal and barrier properties," *Materials Today Communications*, vol. 17, pp. 380–390, 2018.
- [50] B. Li, Y. Sun, J. Yao et al., "An environment-friendly chemical modification method for thiol groups on polypeptide macromolecules to improve the performance of regenerated keratin materials," *Materials & Design*, vol. 217, Article ID 110611, 2022.
- [51] L. Lü, L. Zhang, M. S. M. Wai, D. T. W. Yew, and J. Xu, "Exocytosis of MTT formazan could exacerbate cell injury," *Toxicology in Vitro*, vol. 26, no. 4, pp. 636–644, 2012.
- [52] R. Wang and H. Tong, "Preparation methods and functional characteristics of regenerated keratin-based biofilms," *Polymers*, vol. 14, no. 21, Article ID 4723, 2022.
- [53] I. Sinkiewicz, A. Śliwińska, H. Staroszczyk, and I. Kołodziejaska, "Alternative methods of preparation of soluble keratin from chicken feathers," *Waste and Biomass Valorization*, vol. 8, no. 4, pp. 1043–1048, 2017.
- [54] V. M. Perez-Puyana, A. J. Capezza, W. R. Newson et al., "Functionalization routes for keratin from poultry industry side-streams—towards bio-based absorbent polymers," *Polymers*, vol. 15, no. 2, Article ID 351, 2023.
- [55] S. Isarankura, N. Ayutthaya, and S. Tanpichai, "Keratin extracted from chicken feather waste: extraction, preparation, and structural characterization of the keratin and keratin/biopolymer films and electrospuns," *Journal of Polymers and the Environment*, vol. 23, no. 4, pp. 506–516, 2015.
- [56] T. Tesfaye, B. Sithole, and D. Ramjugernath, "Preparation, characterization and application of keratin based green biofilms from waste chicken feathers," *International Journal of Chemical Science*, vol. 16, 2018.
- [57] N. Ramakrishnan, S. Sharma, A. Gupta, and B. Y. Alashwal, "Keratin based bioplastic film from chicken feathers and its characterization," *International Journal of Biological Macromolecules*, vol. 111, pp. 352–358, 2018.
- [58] M. Brebu and I. Spiridon, "Thermal degradation of keratin waste," *Journal of Analytical and Applied Pyrolysis*, vol. 91, no. 2, pp. 288–295, 2011.
- [59] A. N. M. A. Haque and M. Naebe, "Material extrusion of wool waste/polycaprolactone with improved tensile strength and

- biodegradation,” *Polymers*, vol. 15, no. 16, Article ID 3439, 2023.
- [60] S. de Valence, J.-C. Tille, J.-P. Giliberto et al., “Advantages of bilayered vascular grafts for surgical applicability and tissue regeneration,” *Acta Biomaterialia*, vol. 8, no. 11, pp. 3914–3920, 2012.
- [61] I. Mitra, S. Mukherjee, V. P. Reddy B. et al., “Benzimidazole based Pt(II) complexes with better normal cell viability than cisplatin: synthesis, substitution behavior, cytotoxicity, DNA binding and DFT study,” *RSC Advances*, vol. 6, no. 80, pp. 76600–76613, 2016.
- [62] R. D. B. Fraser and D. A. D. Parry, “The structural basis of the filament-matrix texture in the avian/reptilian group of hard β -keratins,” *Journal of Structural Biology*, vol. 173, no. 2, pp. 391–405, 2011.
- [63] P.-Y. Chen, J. McKittrick, and M. A. Meyers, “Biological materials: functional adaptations and bioinspired designs,” *Progress in Materials Science*, vol. 57, no. 8, pp. 1492–1704, 2012.
- [64] M. Konop, M. Rybka, and A. Drapała, “Keratin biomaterials in skin wound healing, an old player in modern medicine: a mini review,” *Pharmaceutics*, vol. 13, no. 12, Article ID 2029, 2021.
- [65] A. Ghosh, A. Ali, and S. R. Collie, “Effect of wool keratin on mechanical and morphological characteristics of polycaprolactone suture fibre,” *Journal of Textile Engineering*, vol. 63, no. 1, pp. 1–4, 2017.
- [66] S. Y. Kim, B. J. Park, Y. Lee et al., “Human hair keratin-based hydrogels as dynamic matrices for facilitating wound healing,” *Journal of Industrial and Engineering Chemistry*, vol. 73, pp. 142–151, 2019.